THE BULK MINERALOGY AND WATER CONTENTS OF THE CARBONACEOUS CHONDRITE FALLS KOLANG AND TARDA.
A. J. King[1], H. C. Bates[1], P. F. Schofield[1] and S. S. Russell[1] [1]Department of Earth Science, Natural History Museum, London, UK (a.king@nhm.ac.uk).

Introduction: Carbonaceous chondrites offer crucial insights into the abundance, distribution, and transport of volatile species in the early solar system. The low albedo asteroids from which they originate likely played an important role in the delivery of water and organic phases to the terrestrial planets [e.g. 1]. However, carbonaceous chondrites are susceptible to weathering processes and their volatile components are rapidly modified upon entering the Earth's atmosphere [e.g. 2]. Ideally, they are recovered, curated, and analyzed as soon as possible after landing. In 2020 there were two large carbonaceous chondrite falls, Kolang and Tarda, providing an opportunity to investigate volatiles that have experienced minimal exposure to the terrestrial environment.

The Kolang meteorite landed in Indonesia on the 1st August 2020 and ~2.5 kg of material has been collected. In the *Meteoritical Bulletin* interior stones are described as ranging from dark gray to black in color and having a brecciated texture with chondrule-rich and chondrule-poor lithologies [3]. Chondrules are partially to fully hydrated and set within a matrix of phyllosilicates, tochilinite, Fe-sulfides, and carbonates. The mineralogy and oxygen isotopic composition of the average Kolang lithology ($\delta^{17}O$ ~1.75 ‰, $\delta^{18}O$ ~8.47 ‰) led to a CM1/2 classification [3].

On the 25th August 2020, the Tarda meteorite was seen to fall in Morocco, with the first samples collected the following day. Tarda has a total mass of ~4 kg and is a breccia with abundant matrix (~80 vol%) in which small chondrules and chondrule fragments are embedded [3]. The matrix consists of phyllosilicates, magnetite, Fe-sulfides, and carbonates. There are no calcium- and aluminum-rich inclusions (CAIs) but an igneous achondrite clast has been found. The $\delta^{18}O$ composition of separate fragments of Tarda have a bimodal distribution overlapping with the CI ($\delta^{18}O$ ~17 ‰) and CY ($\delta^{18}O$ ~22 ‰) chondrites but with lower $\Delta17O$ values than either group. It is classified as a $C2_{ung}$ chondrite [3].

Here, we have used position-sensitive-detector X-ray diffraction (PSD-XRD) and thermogravimetric analysis (TGA) to characterize the bulk mineralogy and water contents of Kolang and Tarda ~4 months after their fall. We conclude that Kolang is the most altered CM chondrite fall recovered to date, and that Tarda likely formed on a hydrated parent body beyond the orbit of Jupiter.

Experimental: Approximately 200 mg fusion-crust free chips of Kolang and Tarda were powdered and homogenized using an agate mortar and pestle. The powdered meteorites were then loaded into aluminum sample wells (~50 mg) and analyzed using a PSD-XRD at the Natural History Museum (NHM), London. Following our established procedures, diffraction patterns were collected for 16 hours for the meteorites and 30 minutes for standards, and mineral abundances were quantified using a profile-stripping method [4–6].

After the PSD-XRD measurements, ~12 mg of each meteorite powder was analyzed using a TA Instruments SDT Q600 TGA at the NHM. The powder was loaded into an alumina crucible and mass loss recorded as the sample was heated at 10°C/min from room temperature to 1000°C under an N_2 flow. Water contents were determined by assuming that all mass loss between 200 – 800°C was due to the dehydration of -OH/H_2O-bearing phases; this is a slight overestimate as Fe-sulfides, carbonates, and organics also breakdown in this temperature range [7, 8].

Results & Discussion: Figs. 1 and 2 show the PSD-XRD patterns and TGA curves for Kolang and Tarda. Fig. 3 compares their bulk phyllosilicate and water contents to the CI, CM and CY chondrites.

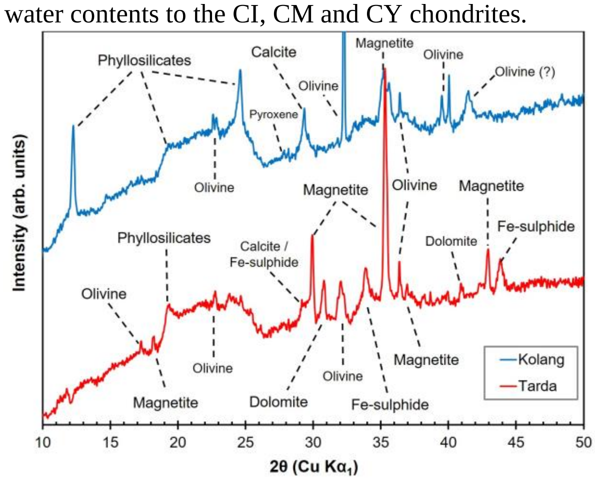

Fig. 1. *PSD-XRD patterns of Kolang and Tarda.*

Kolang. Kolang is comprised of phyllosilicates (82 vol%), olivine (8 vol%), pyroxene (5 vol%), magnetite (3 vol%), Fe-sulfides (1 vol%) and calcite (1 vol%). Tochilinite was not detected by PSD-XRD. We concur with a CM1/2 classification; Kolang has a phyllosilicate fraction (PSF) of 0.86, which corresponds to a petrologic sub-type of 1.3 on the scale of Howard et al. [5] and 2.2 on the scale of Rubin et al. [9]. The TGA derived water abundance is ~13 wt% and while Kolang is a breccia, Fig. 3 confirms that its bulk mineralogy and water contents are consistent with the most altered altered CM chondrites [6, 10].

Other highly altered CM chondrites have relatively low $\delta^{18}O$ values (~2 – 6 ‰) [11]. The oxygen isotopic composition of Kolang's average lithology plots in the middle of the CM field and is heavier than all other CM1/2 and CM1 chondrites (excluding several hot desert meteorites), although the composition of our Kolang powder is yet to be determined. Models predict heavier oxygen isotopic compositions with increasing alteration by $\delta^{18}O$-rich fluids [e.g. 12]. Previously analyzed CM1/2 and CM1 chondrites were desert finds, and their low $\delta^{18}O$ values might be explained by terrestrial contamination [11]. Kolang is the most aqueously altered CM chondrite fall and has experienced negligible weathering, so further studies of this meteorite will be important to establish the relationship between alteration and oxygen isotopes on primitive asteroids.

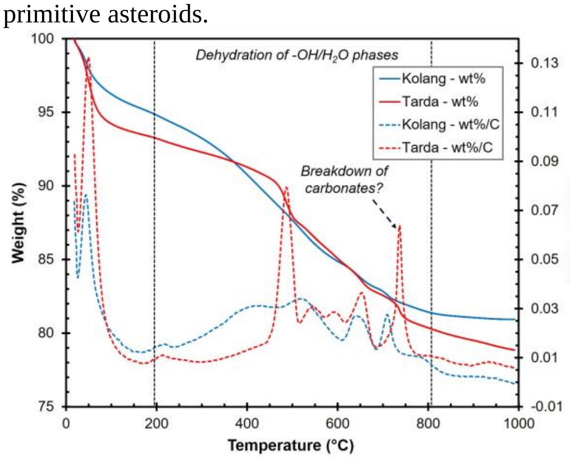

Fig. 2. TGA mass loss curves for Kolang and Tarda.

Tarda. Tarda consists of phyllosilicates (72 vol%), olivine (10 vol%), magnetite (8 vol%), Fe-sulfides (8 vol%) and dolomite (2 vol%), giving a PSF of 0.88 and a petrologic sub-type of 1.3. The PSD-XRD pattern of Tarda is comparable to the CI chondrites but its TGA mass loss curve is different [8, 13]; sulphates and Fe-(oxy)hydroxides are absent, and the profile of the curve suggests that the phyllosilicates may belong to the chlorite-group (e.g. chamosite and clinochlore). The estimated water abundance is ~13 wt%.

Based on its mineralogy and water contents we agree that Tarda is distinct from the CI chondrites. It also differs from the CY chondrites, whose heavy oxygen isotopic compositions have been attributed to thermal metamorphism at temperatures >500°C [14]. We find no compelling evidence for phyllosilicate dehydration and recrystallisation in Tarda.

The oxygen isotopic composition of Tarda is similar to that of WIS 91600 ($\delta^{18}O$ ~17 ‰), an unusual heated (~400–500°C) and magnetite-rich (~9 vol%) CM_{an} chondrite believed to have formed at ~10 AU [15]. However, considering both isotopic and mineralogical characteristics, we suggest that Tarda is a $C1/2_{ung}$ chondrite most closely related to the unique $C2_{ung}$ Tagish Lake ($\delta^{18}O$ ~18 ‰). The bulk mineralogy of Tagish Lake includes phyllosilicates (71 vol%), Fe-Mg carbonates (12 vol%), olivine (7 vol%), magnetite (5 vol%) and Fe-sulfides (5 vol%) [4]. The Tagish Lake parent body is estimated to have formed at ~8 – 13 AU [16]. Tarda is also likely a sample from the outer regions of the solar system, a hypothesis that will be tested by upcoming infrared (IR) measurements.

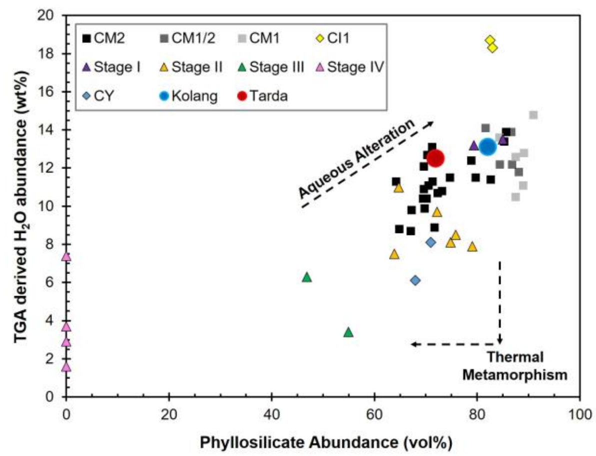

Fig. 3. Phyllosilicate and TGA derived water abundances for Kolang and Tarda compared to CI, unheated and heated (Stages I–IV) CM, and heated CY chondrites. Data are taken from [6, 8, 10, 13, 17, 18].

References: [1] Alexander C. M. O'D. et al. (2012) *Science, 337*, 721–723. [2] King A. J. et al. (2020) *GCA, 268*, 73–89. [3] Meteoritical Bulletin, #109 (in prep). [4] Bland P. A. et al. (2004) *M&PS, 39*, 3–16. [5] Howard K. T. et al. (2015) *GCA, 149*, 206–222. [6] King A. J. et al. (2017) *M&PS, 52*, 1197–1215. [7] Garenne A. et al. (2014) *GCA, 137*, 93–112. [8] King A. J. et al. (2015) *Earth, Plan. Spa., 67*, 198. [9] Rubin A. E. et al. (2007) *GCA, 71*, 2361–2382. [10] Bates H. C. et al. (2020) *M&PS, 55*, 77–101. [11] King A. J. et al. (2018) *49th LPSC*, #2201. [12] Clayton R. N. & Mayeda T. K. (1999) *GCA 63*, 2089–2104. [13] King A. J. et al. (2015) *GCA, 165*, 148–160. [14] King A. J. et al. (2019) *Geochem., 79*, 125531. [15] Bryson J. F. J. et al. (2020) *ApJ, 896*, 103. [16] Bryson J. F. J. et al. (2020) *ApJ, 892*, 126. [17] King A. J. et al. (2020) *51st LPSC*, #1883. [18] King A. J. et al. (2021) *GCA* (in revision).